**Direct Membrane Filtration (DMF) of municipal wastewater by mixed matrix membranes (MMMs) filled with graphene oxide (GO): towards a circular sanitation model**

Eduardo L. Subtil[a*]; Rodrigo Almeria Ragio[a]; Hugo G. Lemos[a]; Gidiane Scaratti[a]; Joan García[b]; Pierre Le-Clech[c]

[a]Center of Engineering, Modeling and Applied Social Sciences, Federal University of ABC, Santo André/SP, Brazil.

[b]GEMMA-Group of Environmental Engineering and Microbiology, Department of Civil and Environmental Engineering, Universitat Politècnica de Catalunya-BarcelonaTech, Barcelona, Spain.

[c]UNESCO Centre for Membrane Science and Technology, School of Chemical Engineering, The University of New South Wales, Sydney, Australia

*Corresponding author: eduardo.subtil@ufabc.edu.br, Av. dos Estados, 5001, São Paulo, 09210-580, Brazil.

**Abstract**

Direct membrane filtration (DMF) is an emerging wastewater treatment technology for providing high-quality effluents as well as efficient organic waste recovery from the concentrate. The latter may then be used for methane production, a renewable energy source. However, widespread application of DMF in large systems still faces challenges due to fouling effects. In this work, polyethersulfone-graphene oxide (PES-GO) ultrafiltration membranes were successfully synthesized by phase-inversion and applied for the first time in a DMF system for a real municipal wastewater. The incorporation of GO resulted in membranes showing increased flux recovery, higher rejection capacity and enhanced irreversible fouling resistance which could be mainly attributed to their more hydrophilic and restrictive selective layer. More specifically, PES-GO(0.6%) membrane reached 91% of flux recovery, indicating a substantial improvement in the membrane reusability when compared to PES membrane. The findings of cake layer characterization confirm that changes in the membrane surface caused by the addition of GO allowed for a reduction in protein deposition, and that its contribution to fouling formation during DMF is greater than carbohydrates. Thereby, these results show promising features for GO modified membranes in DMF systems aiming organic matter recovery for self-energy sustainable wastewater treatment plants.

**Keywords:** resource recovery, ultrafiltration, foulants, methane, water reuse, nanomaterials, graphene oxide

## 1. Introduction

World is facing with an unprecedented challenge to overcome the trade-off of meeting rising demand with less resources, without compromising water, energy and food security. On the other hand, tons and tons of sewage produced daily, with a high amount of water, energy and nutrient, are treated as waste and discharged into the environment. Therefore, the development of new technologies, designs and flow sheets for municipal wastewater treatment plants (WWTPs) based on an interdisciplinary approach is critical for the successful paradigm shift from wastewater disposal issue to resource recovery solution, towards a circular economy model.

Significant advances have been made during the last decade in the development of resource-oriented technologies for wastewater treatment [1–4]. Among them, Direct Membrane Filtration (DMF) is emerging as an innovative concept [5]. In this new conception, the organic content of raw wastewater is pre-concentrated by driven-pressure membrane for further anaerobic degradation, resulting in a high yield methane production, making it economically feasible for energy recovery [6,7]. In addition, the permeate produced by the membrane can be directly reused (i.e., for irrigation) or further treated for advanced water reuse or nutrients recovery [8]. While previous works have found significant results regarding methane production and effluent quality [9,10], the absence of DMF technology in the market is greatly hampered by fouling which has a significant impact on operating costs [8,11].

During pre-concentration of wastewater, membranes are exposed to high contents of hydrophobic organic matter, particles and microorganisms (membrane foulants) from raw wastewater [12]. Due to the hydrophobic and rough characteristics of commercially available polymeric membranes (i.e.; Polyethersulfone - PES, polyvinylidene fluoride-PVDF), high physicochemical interaction with the foulants is expected [13,14].

Therefore, a significant short-term flux reduction because of the large adsorption/deposition of material on the membrane surface and pores is expected to occur at constant transmembrane pressure operation [15,16]. Although physical and chemical approaches to minimize fouling in DMF system, such as pretreatment by coagulation and flocculation [12,17,18], chemically enhanced backwash and aeration [11,19,20], have been proposed and tested, these methods result in increased operational costs. In addition, these approaches can generate secondary contaminants, reduce the production potential of methane from the concentrate (less energy recovery) and shorten the lifetime of the membranes [8]. Consequently, the next step in making DMF a feasible resource-oriented technology is the development of new membranes with antifouling properties. The significance of this topic is further supported by a recent literature review on DMF for wastewater treatment and resource recovery [8]. The authors stated that the use of membranes with improved antifouling properties, as well as identifying membrane fouling mechanisms and dominant foulants, is crucial and necessitates extensive research.

There is now considerable evidence that the use of nanoparticles can significantly alter the physicochemical properties of polymeric membranes (i.e., hydrophilicity, pore size, porosity, surface charge, membrane stability) and improve fouling resistance [21–23]. Subtil et al. [13] founded a remarkable irreversible fouling suppression for organic compounds by adding two nanoparticles (polyaniline and reduced graphene oxide) as additives in polymeric UF membranes. Many of these nanofillers are particularly hydrophilic (i.e., graphene oxide (GO), titanium oxide), thereby easily spread in polymeric solutions.

In recent years, the use of GO as additive in the synthesis of polymeric mixed matrix membranes has received much attention [24–26]. The presence of hydrophilic and negatively charged functional groups in their 2D nanosheets can make the membrane

selective layer more hydrophilic and less rough, which is required to prevent irreversible deposition of hydrophobic organic compounds and increase their rejection [27,28]. Jin et al. [29] incorporated GO into the PES polymer matrix to improve hydrophilicity and antifouling ability of the PES membrane. Using a bovine serum albumin (BSA) solution, the authors discovered that adding GO increased membrane flux while decreasing protein static adsorption. Igbinigun et al. [30] proposed a different approach in which GO nanosheets were spin coated onto the polyallylamine modified membrane surface to reduce organic fouling. The antifouling ability of the membranes was evaluated by using humic acid solution as a single foulant and they found that the modified PES membrane had relatively smooth surface and exhibited 2.6 times greater flux recovery than an unmodified PES-UF membrane.

Despite studies on GO for the synthesis of hydrophilic mixed membranes have recently been carried out, its application and evaluation for recovery of organic content from urban wastewater has yet to be investigated. This is especially important given that GO-based membranes performance is strongly linked to the effluent characteristics, and raw wastewater contains a high concentration of suspended solids and organic compounds that combined with inorganic substances cause more severe fouling than other effluent matrices[6,8]. For instance, Lemos et al. [14] demonstrated that the fouling rate and cake layer development of GO-incorporated membranes for the treatment of landfill leachate and domestic wastewater were significantly lower than in previous studies that used only domestic wastewater. The authors also demonstrated that, while the GO membrane outperformed the PES control membrane in terms of flow decay and humic substance rejection using single model foulant solutions, there were no significant differences observed during MBR operation with leachate due to high concentrations of humic substances and extracellular polymeric substances.

Aside from fouling issues, to enable efficient energy recovery, the organic content of municipal wastewater must be concentrated as much as possible, since a Chemical Oxygen Demand (COD) > 1500 mg/L is desirable for anaerobic digestion [31]. Ultrafiltration (UF) membranes can efficiently reject large organics while allowing smaller ones to pass through. For this reason, increasing the rejection capacity of membranes during wastewater filtration is a key step for the energetic feasibility of this new approach. To achieve high organic matter rejection, forward osmosis (FO) has been used in DMF applications. However, the draw solution regeneration [32], low concentration factor, and sulfate retention in the concentrate which cause serious problems for anaerobic digestion (i.e., toxicity, odor, and reduced methane production) are significant drawbacks [6,33,34]. On the other hand, increased amounts of GO in the membrane separating layer can improve separation capability of porous membrane by enhancing the exclusion mechanism, while reducing the effect of fouling-induced flow loss [14].

In this work, polyethersulfone-graphene oxide (PES-GO) ultrafiltration (UF) membranes is to be synthesized by phase-inversion and applied for the first time for fouling reduction and organic matter recovery during direct filtration of urban wastewater. Different from previous research, larger amounts of GO in the polymer solution were investigated to improve the rejection capacity of mixed matrix membranes (MMMs). Membranes were characterized in terms to morphology, composition, surface hydrophilicity and water permeability. Furthermore, filterability tests were performed with effluent collected in a WWTP to evaluate the pollutants rejection capacity and organic matter concentration of the membranes, as well as the characterization and quantification of fouling.

## 2. Materials and methods

### 2.1. Materials

Polyethersulfone (PES, molecular weight (MW) of 63,000 g.mol$^{-1}$) was acquired from Solvay. N-Methyl-2-pyrrolidone (NMP) (anhydrous, 99.5%) was provided by LabSynth. The GO was synthesized according to a modified Hummer's method [35] . Spectroscopic and morphological analyses were performed to confirm the successful obtaining of the 2D material (Supplementary Information, Figures S1 and S2).

### 2.2. Membrane synthesis and characterization

Polyethersulfone was chosen for this study because it is recognized as a high-performance, easy-to-process polyaromatic polymer for the synthesis of porous membranes with good chemical resistance, a wide temperature range, and a pH tolerance [36,37]. As a result, PES is widely used to produce Microfiltration (MF) and Ultrafiltration (UF) membranes among the various polymers used for membrane synthesis [38].

The PES/GO membranes were obtained by phase inversion process via immersion precipitation, as described in previous work [14] . Briefly, exfoliated GO was dispersed in NMP solutions using a probe sonicator. Then, PES was slowly poured into GO dispersions and stirred for 24 h using a mechanical stirrer. A pure PES casting solution was also obtained for comparison. Table 1 shows the mass fractions of polymer and GO for PES and PES-GO casting solutions. After sonication for 2 h to remove gas bubbles, the solutions were cast on a glass plate with an automatic film applicator (Elcometer 4340) followed by their immersion in an ultrapure water coagulation bath.

The membranes were previously immersed in isopropyl alcohol for 24 h and dried at room temperature before characterization. Morphological analysis of the membranes was performed by scanning electron microscopy (SEM) using a JEOL JSM-6010LA

microscope. In order to investigate the internal porous structure of the samples, cross-section surfaces of the membranes were obtained by breaking them after their immersion into liquid nitrogen. For the Raman spectroscopy, spectra were collected from the dried membranes top-surfaces using a Horiba-Jobin-Yvon T64000 spectrometer operating with a Laser-Verdi-G5 (532 nm). The laser excitation source was maintained below 1 mW and focused on the samples with a 50x objective. At least, three different regions were characterized for each sample.

An effective method for characterizing surface properties is to analyze the surface energy and affinity of the liquid for the membrane. Wettability or hydrophilicity, in particular, has a significant impact on permeability, fouling type, and membrane self-life. In this study, the hydrophilicity of the synthesized membranes (i.e., PES and PES-GO) was estimated based on optical drop shape method by the sessile drop techniques in its dry state at room temperature [39]. An optical contact angle goniometer was employed (model SL150E - USA KINO). In a summary, a drop of deionized water was deposited on the flat surface of the dried membrane, and the static contact angle of the drop with the surface was measured. Three pieces of each membrane were used to estimate the contact angle, and five measurements of each sample were taken. A gravimetric method was used to determine membrane porosity [40]. An electronic micrometer was used to estimate the thickness of each membrane from five different pieces (Digimess, 0-25mm 0.001mm) and then used to determine the porosity according to Equation 1.

$$\mathrm{P}(\%) = \frac{\frac{m_1 - m_2}{\rho_w}}{V_m} \cdot 100 \qquad (1)$$

Where $m_1$ is the membrane wet weight, $m_2$ is the membrane dry weight, $\rho_w$ is the specific density of water and $V_m$ is the membrane volume obtained from the thickness (m) and area ($m^2$).

**Table 1**: Casting solution composition.

| Membrane | PES (wt%) | NMP (wt%) | GO (wt%) |
|---|---|---|---|
| PES | 17.0 | 83.0 | - |
| PES-GO(0.3%) | 17.0 | 82.7 | 0.3 |
| PES-GO(0.6%) | 17.0 | 82.4 | 0.6 |

### 2.3. Membrane rejection and organic matter concentration

The feed (i.e., domestic wastewater collected in a municipal WWTP) permeate and retentate were characterized according to the physico-chemical analyses reported in Table S1, to evaluate membrane rejection and sewage concentration. The analyses were performed following the procedures in Standard Methods for the Examination of Water and Wastewater [41], except for carbohydrates [42] and proteins [43] which were analyzed using Lowry method and sulfuric acid-UV method, respectively, and dissolved nitrogen (DN), that was evaluated using a total organic carbon analyzer coupled with an TN unit TNM-L (TOC-$L_{CPH}$ Shimadzu). Prior to dissolved organic carbon (DOC) and DN filtrate analysis, samples were vacuum filtrated through 0.45 μm acetate cellulose filters.

### 2.4. Fouling assessment

#### 2.4.1. Membrane cell test and filterability assays

For filterability tests, a crossflow filtration cell with 85.1 $cm^2$ membrane area was used (Fig. 1) [44]. The experiments were performed at room temperature (21.9 ± 0.6 °C) and constant transmembrane pressure (0.7 bar). Each filtration cycle consisted in membrane compaction with deionized water at 1 bar (TMP), following $J_{w1}$ initial deionized water filtration, $J_S$ sample filtration until 50% recovery rate was achieved (initial sample

volume: 1 L) and two deionized water filtrations, the first without cleaning the membrane ($J_{w2}$) and the second after physically cleaning the membrane with a bushing ($J_{w3}$). Other sample filtration was carried out to evaluate the membrane reusability until a 50% recovery rate was achieved.

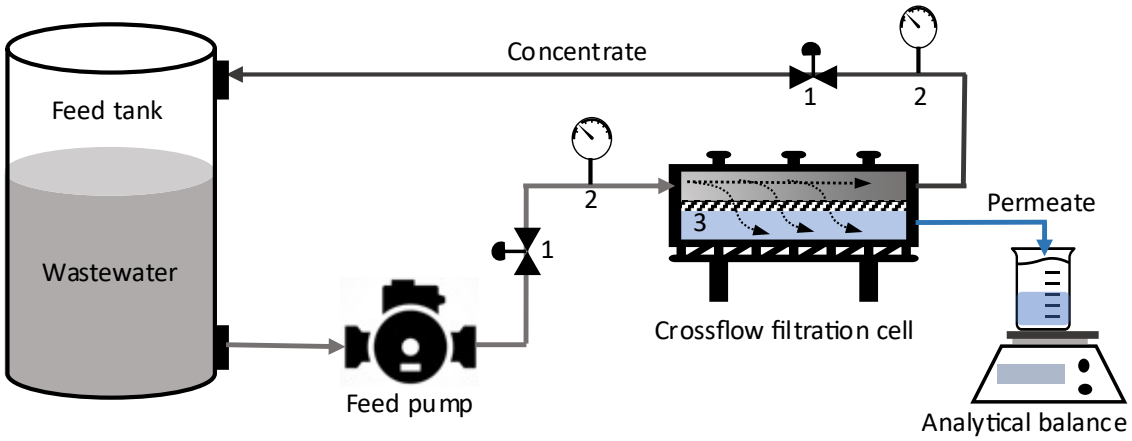


**Figure 1:** Schematic diagram of crossflow filtration, where: 1) needle valve; 2) manometer and 3) flat sheet membrane.

The mass of the permeate was quantified using an analytical balance (AUW220D, Shimadzu). The corresponding volume was determined using the water specific mass (998 kg $m^{-3}$ at 20 °C) and then the flux was calculated with Equation 2:

$$J = \frac{V}{A \times t_j} \quad (2)$$

Where V is the permeate volume (L), A the membrane area ($m^2$) and $t_j$ time between measures (h). Normalized flux was calculated using ratio between initial flux and each flux measured.

### 2.4.2. Fouling analysis

Fouling analyses were performed with different approaches for evaluation of filtration data. Resistance in series (RIS) model were used to quantify resistances attributed to fouling fractions [45] . The standard and the classical cake filtration models

were also applied to evaluate which fouling fraction governed the filtration and was mainly responsible for flux decrease [46] .

Flux recovery ratio (FR) (Equation 3) and fouling ratios (Equations 4-6) were obtained according to Vatanpour *et al.* [47], for better evaluation of reversibility. Higher FR values indicate that physical cleaning was able to recover a larger flux percentage.

$$FR(\%) = \left(\frac{J_{w3}}{J_{w1}}\right) X100 \quad (3)$$

Total fouling ratio ($R_t$) was defined and calculated according to Equation 4:

$$R_{t\%} = \left(1 - \frac{J_s}{J_{w1}}\right) X100 \quad (4)$$

Where $R_t$ indicates the degree of total flux loss caused by fouling.

Reversible fouling ratio ($R_r$) and irreversible fouling ratio ($R_{ir}$) were defined and calculated using Equations 5 and 6, with $R_t$ as the sum of $R_r$ and $R_{ir}$:

$$R_{r\%} = \left(\frac{J_{w3} - J_s}{J_{w1}}\right) X100 \quad (5)$$

$$R_{ir\%} = \left(\frac{J_{w1} - J_{w3}}{J_{w1}}\right) X100 \quad (6)$$

Fouling mechanisms was determined according to RIS model, using Equations 7-10. In this work, total resistance ($R_t$) was divided in membrane resistance ($R_m$) and three resistances whose sum is the fouling resistance ($R_f$), the resistance by the pore blockage fraction ($R_b$), that included resistance by remaining fouling after physical cleaning, concentration polarization fraction ($R_{cb}$) and cake layer fraction ($R_c$). Most physical cleaning methods were expected to remove most of the cake layer, which is referred to as reversible fouling [48]. As a result, in addition to pore blocking (complete and standard blocking), the residual fraction from the cake layer was considered mostly irreversible fouling, a reminiscent after physical cleaning. However, because the cake layer is mostly made up of particles bigger than the membrane pores, only a small portion of this surface deposit is predicted to contribute to irreversible fouling and is often overlooked [49].

Based on these previous reports, in this study, reversible fouling is here referred to the fraction of the cake layer that can be removed by physical cleaning, abbreviated as $R_c$, whereas irreversible fouling includes pore blocking (complete and standard) as well as the remaining surface fraction of the cake layer, all of which are abbreviated as $R_b$. Concentration polarization refers to the layer of solutes accumulated near membrane surface due to their rejection on the course of filtration, being responsible for increasing filtration resistance [50] and merely replacing the feed solution with DI water is enough to remove such accumulation and evaluate its contribution to $R_t$.

$$R_t = \frac{TMP}{\eta\, J_s} = R_m + R_b + R_c + R_{cb} = R_m + R_f \quad (7)$$

$$R_{cb} = \frac{TMP(J_{w2} - J_s)}{\eta\, J_s J_{w2}} = \frac{\Delta P_t}{\eta\, J_s} - (R_m + R_b + R_c) \quad (8)$$

$$R_c = \frac{TMP(J_{w3} - J_{w2})}{\eta\, J_{w2} J_{w3}} = \frac{TMP}{\eta\, J_{w2}} - (R_m + R_b) \quad (9)$$

$$R_b = \frac{TMP(J_{w1} - J_{w3})}{\eta\, J_{w3} J_{w1}} = \frac{TMP}{\eta\, J_{w3}} - R_m \quad (10)$$

Where TMP is the transmembrane pressure (bar), J is the flux at the related filtration stage (L $m^2$ $h^{-1}$) and η is permeate dynamic viscosity (Pa s).

Standard filtration (t/V-t) (Equation 11) and the classical cake filtration (t/V-V) (Equation 12) models were evaluated by adjusting sample filtration data, which corresponds for fouling caused by particles smaller than membrane pores (flow reduced owing to pore clogging), and fouling caused by particles larger than membrane pores (development of a cake layer on the membrane surface), respectively.

$$\frac{t}{V} = \frac{1}{Q_0} + \frac{k}{2} t \quad (11)$$

Where t is filtration time (min), V is accumulated permeate volume (L), $Q_0$ is initial flow (L.$min^{-1}$) and k is a filtration constant ($L^{-1}$).

$$\frac{t}{V} = \frac{\mu . R_m}{A \cdot TMP} + \frac{\mu . c . R_c}{2A^2 \cdot TMP} V = \frac{1}{Q_0} + \frac{K}{2} V \quad (12)$$

Where μ is dynamic viscosity (Pa s), $R_m$ is membrane resistance ($m^{-1}$), A is membrane area ($m^2$), c is particle concentration (kg $L^{-1}$), $R_c$ is cake layer resistance (m $kg^{-1}$), TMP is transmembrane pressure (Pa) and K is cake filtration constant (min $L^{-2}$).

### 2.4.3. Characterization of the fouled membrane

Morphological and spectroscopic analyses of the fouled membranes were performed by SEM and Fourier-transform infrared spectroscopy (FTIR), respectively. The FTIR was carried out using a Varian 640-IR FT-IR spectrometer operating with an attenuated total reflectance (ATR) accessory. The amount of proteins and carbohydrates accumulated in membrane surface was also evaluated. A fouled membrane piece of 2 x 7 cm was separated, cut into smaller pieces, and put in a beaker with 25 mL of DI water and a magnetic stirred for 3 min. After stirring, the solution with foulants was separated from the membrane pieces and analyzed in terms of carbohydrates [42] and proteins [43].

## 3. Results and discussion

### 3.1. Membrane characterization

The incorporation of GO into PES matrix was assessed by Raman spectroscopy analysis. Figure 2 shows Raman spectra of only GO and membranes (PES and PES-GO). Raman spectrum of PES shows the characteristic polymer peaks at 1071 and 1105 $cm^{-1}$ ascribed to the symmetric and asymmetric stretching vibrations of O=S=O groups, as well as the strong peak at 1147 $cm^{-1}$ corresponding to the C-O-C stretching. PES Raman spectrum also exhibits broad bands at 1580 and 1601 $cm^{-1}$ related to the phenyl structures [40]. Likewise, Raman spectrum of GO shows the characteristic D and G bands at 1350 and 1590 $cm^{-1}$, respectively. The G band refers to the inherent $sp^2$ hybridized carbon bonds of graphene pristine, whereas the D band corresponds to the $sp^3$ hybridized carbon bonds resulted from attached hydroxyl, ether and carboxylic functionalities after oxidation process. The favored dispersion of GO into PES matrix could be confirmed by the strong

presence of the GO bands at PES-GO membranes spectra. It has been knwon that the high number of polar funcionalities from GO contributes to enhance their interaction with PES mainly by hydrogen bonds [40]. Also, the digital pictures obtained with different GO concentrations display uniform colors, which gradually changes from white to gray with the increase of GO concentration, indicating that GO nanoparticles are dispersed into the MMMs homogeneously.

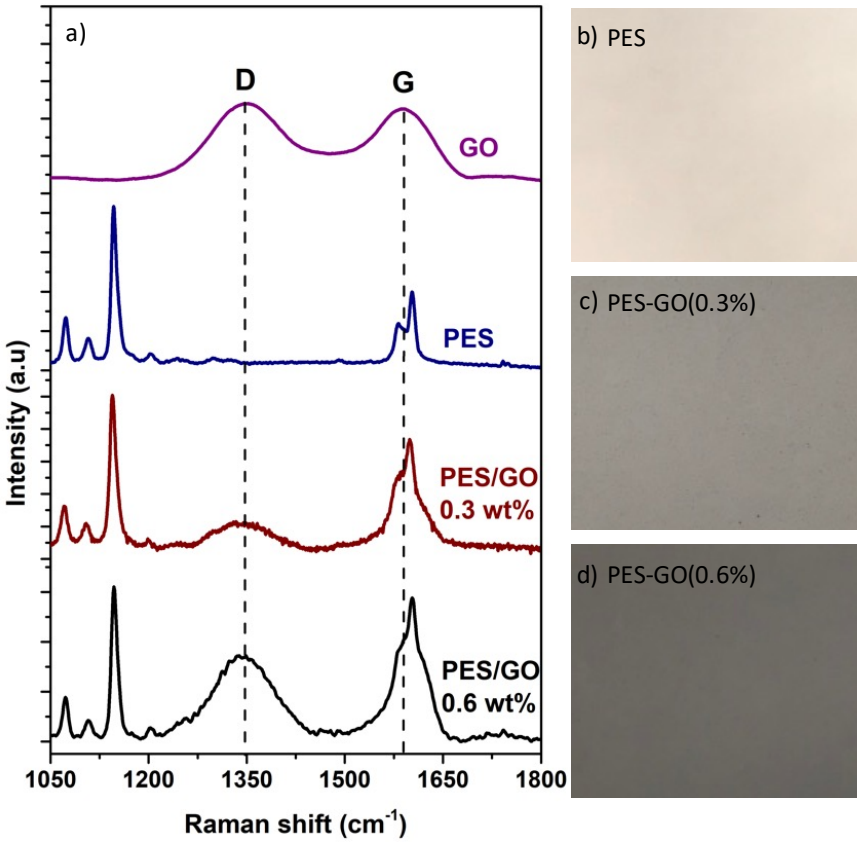


**Figure 2**. (a) Raman spectra of GO, PES and PES-GO membranes, where D and G correspond to the characteristics bands of GO. (b-d) Respective digital pictures of PES and PES-GO membranes.

The reduced porosity and mean pore size as well as the increased skin layer thickness showed by PES-GO membranes had an impact on their permeability (Table 3). Permeability dropped from 290 ± 37 $L.m^{-2}.h^{-1}.bar^{-1}$ (PES) to 105 ± 6 $L.m^{-2}.h^{-1}.bar^{-1}$ [PES-GO(0.3%)] due to the increased water transport resistance across the membrane. On the

other hand, higher concentration of GO contributed to increase PES-GO(0.6%) wettability resulting in slightly enhanced membrane permeability (120 ± 2 $L.m^{-2}.h^{-1}.bar^{-1}$). This phenomenon could be observed through the decreased contact angle of PES-GO membranes and is mainly attributed to the higher concentration of hydrophilic groups from GO which enhances the interaction between the water molecules and the membrane pore structure, favoring a larger uptake of water molecules and a higher membrane wettability [24].

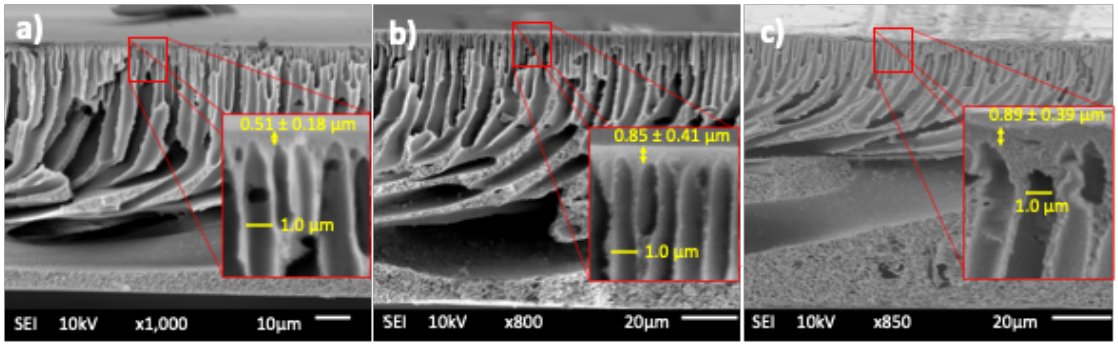


**Figure 3**: SEM images of membrane cross-section of PES (a), PES-GO(0.3%) (b) and PES-GO(0.6%) (c).

**Table 3.** Average values of porosity, mean pore size, skin layer thickness, contact angle and permeability for PES and PES-GO membranes.

| **Parameters** | **PES** | **PES-GO(0.3%)** | **PES-GO(0.6%)** |
|---|---|---|---|
| Porosity (%) | 66.1 ± 1.4 | 64.2 ± 1.7 | 60.4 ± 1.2 |
| Mean pore size (nm) | 40 | 29 | 30 |
| Skin layer thickness (µm) | 0.51 ± 0.18 | 0.85 ± 0.41 | 0.89 ± 0.39 |
| Contact angle (º) | 60.1 ± 1.3 | 53.9 ± 1.8 | 47.1 ± 1.4 |
| Permeability ($L.m^{-2}.h^{-1}.bar^{-1}$) | 290 ± 37 | 105 ± 6 | 120 ± 2 |

### 3.2. Membrane rejection, permeate quality and COD concentration

The effects of the morphology, hydrophilicity and permeability features on the filterability and rejection efficiency of the membranes were analyzed (Table 4 and Figure 4). In general, PES-GO membranes exhibit higher rejection capacities when compared to the PES specimen. Table 4 shows an enhanced reduction of the permeate turbidity for PES-GO membranes which is related to their smaller pores size (Table 3) and consequent better size exclusion capacity. In addition, PES-GO membranes show superior decrease on true color and $Abs_{254}$. While the PES membrane reduced color and humic substances by only 31% and 35%, respectively, the MMMs were able to achieve mean removals of more than 73% for color and up to 51% for $Abs_{254}$.

**Table 4.** Wastewater and permeates physical-chemical characterization.

| **Parameters** | **Wastewater** | **PES** | **PES-GO(0.3%)** | **PES-GO(0.6%)** |
|---|---|---|---|---|
| Turbidity (NTU) | 70.6 ± 2.3 | 1.4 ± 0.3 | 0.4 ± 0.1 | 0.3 ± 0.1 |
| Color (uC) | 169.1 ± 6.2 | 116.8 ± 3.6 | 46.1 ± 8.9 | 42.5 ± 1.5 |
| $Abs_{254}$ (10 x $cm^{-1}$) | 3.40 ± 0.04 | 2.21 ± 0.02 | 1.66 ± 0.02 | 1.81 ± 0.02 |
| COD* | 214.0 ± 7.4 | 27.5 ± 5.7 | 29.5 ± 11.2 | 21.1 ± 7.9 |
| DOC* | 27.2 ± 0.1 | 16.6 ± 0.6 | 12.9 ± 0.3 | 13.5 ± 0.3 |
| Proteins* | 39.1 ± 1.1 | 7.7 ± 1.5 | 4.6 ± 1.3 | 5.2 ± 1.0 |
| Carbohydrates* | 14.5 ± 2.3 | 1.4 ± 0.2 | 0.4 ± 0.2 | 0.4 ± 0.2 |

* mg/L

Analyses of DOC, proteins, carbohydrates, and COD were carried out to evaluate organic compounds rejection efficiency (Table 4 and Fig. 4). Higher proteins rejection and, in particular, higher carbohydrates rejection were obtained for PES-GO membranes than for PES membranes, which could have a positive effect as pretreatment for high-pressure RO processes for non-potable drinking water production, assisting in the long-

term sustainable operation of the RO process. Furthermore, PES-GO membranes outperformed PES membranes in DOC removal, being 13% and 11% higher for PES-GO(0.3%) and PES-GO(0.6%), respectively. Since municipal wastewater may contain a large percentage of dissolved organic substances with low molecular weight (i.e., less than 1000 Daltons) [51], these results suggest that the addition of GO modified the physicochemical properties of the membranes and favors other separation mechanisms that go beyond just size-difference exclusion. It may have contributed to a reduction in the amount of organic contaminants with low molecular weight that passes through the UF membranes, and thus decreased DOC from permeate.

Indeed, the presence of GO results in diminished electrostatic and hydrophobic interactions between the membrane and negatively charged organic compounds of the influent, with some mechanisms acting together for this [14]. GO addition in MMMs is associated with increased humic substances removal, a pollutant associated to color and $Abs_{254}$ in water [52]. Algamdi et al. [53] achieved removal of 95-98% of humic substances (10 to 100 mg/L solutions) for PES-GO membranes (1-5%wt. GO content, relative to %wt. PES) and reduction of humic acid solution adsorption for 1-4%wt GO content in membranes. Such results were attributed to the formation of a hydration layer (produced by -OH and -COOH groups in GO) that reduced interaction between these hydrophobic pollutants and the hydrophobic PES. Beyond the hydration layer, Igbinigun et al. [30] showed that the more negative zeta potential of PES-GO allowed better repulsion between humic compounds and the membrane itself, promoting better retention and less fouling. Such benefits are also expected to allow better retention of proteins, as indicated by Hu et al. [54], who achieved 99.3-99.4% of BSA rejection, for a 1 g/L solution, with a MMM made of PES, sulfonated polysulfone, PEG and GO (0.004-0.016wt. %).

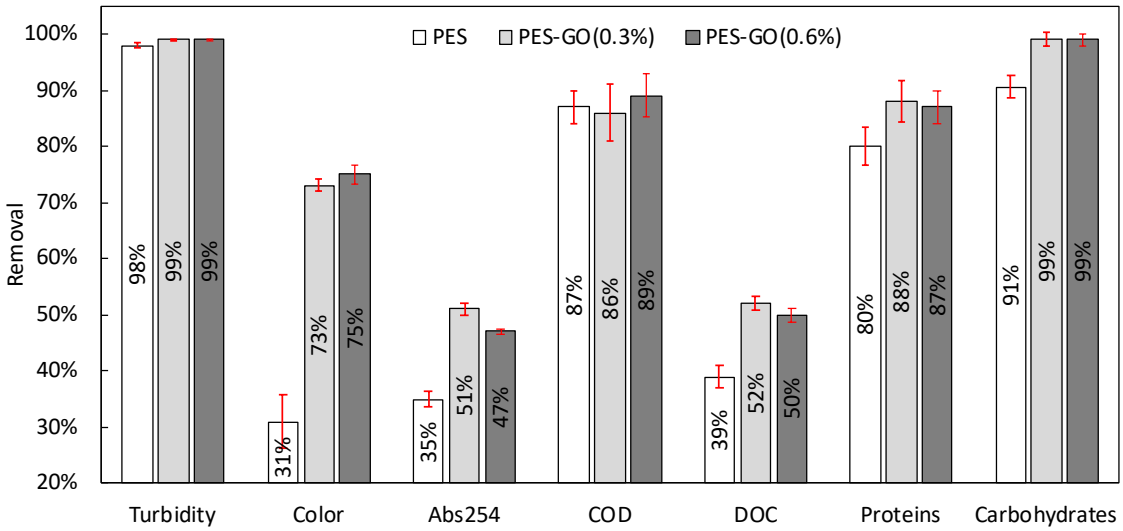


**Figure 4:** Average pollutant removal for PES and PES-GO membranes.

PES and PES-GO membranes exhibit a high COD reduction (>86%), with no significant differences, demonstrating high filterability efficiency by producing permeate with average COD less than 30 mg/L (Table 4). Compared to commercial membranes used for wastewater treatment and organic matter concentration, these PES-GO membranes achieved similar or better COD removal. For instance, Gong et al. [55] achieved 30.9-37.6 mg COD/L in permeate with a commercial PVDF-UF membrane, whereas Ortega-Bravo et al. [56] achieved 49 mg COD/L in permeate with a commercial PES-UF membrane.

The improved performance of PES-GO membranes for dissolved and colloidal organics (i.e., color, $Abs_{254}$, and DOC) opens the potential of improving organic micropollutant removal during DMF, allowing for better permeate quality to meet more stringent legislation for water disposal and reuse. This is a critical aspect of DMF because there is no other integrated process for removing these compounds, and solute-foulants and solute-solute interactions, as well as effluent-membrane interactions, play a major role in micropollutant removal.

The efficiency of PES and PES-GO membranes in organic content concentration was assessed using COD measurements in a single cycle with a sample volume of 1 L. As shown in Figure 5, COD in the concentrate increased significantly with the increasing of permeate recovery from 80% to 90%. For PES-GO(0.6%) membrane, COD concentrate increased from 985.6 mg/L to 1950 mg/L (concentration factor increased from 4.5 to 8.8), for 80% and 90% of permeate recovery, respectively.

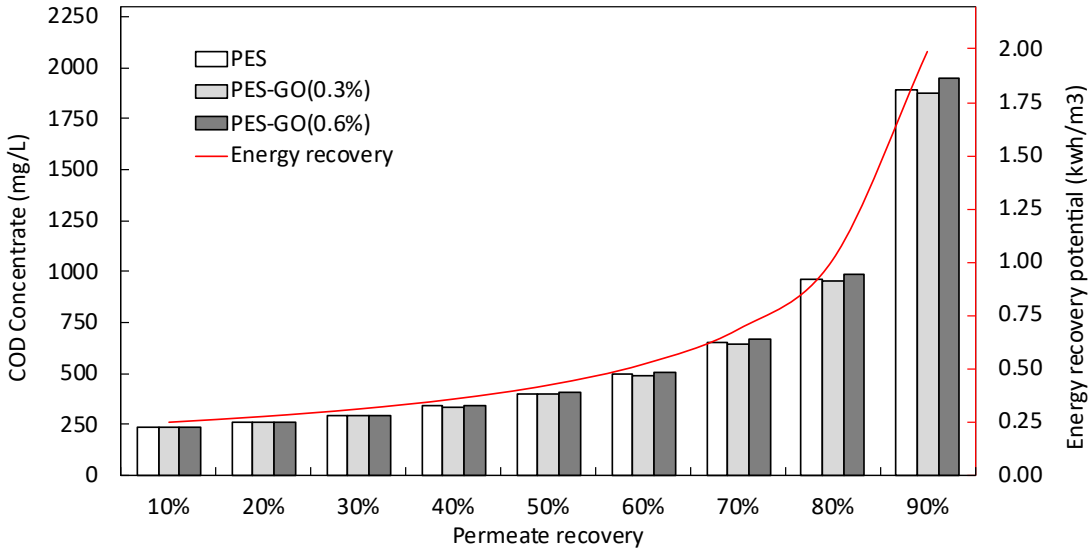


**Figure 5.** COD in the concentrate stream as a function of concentration factor and energy recovery potential, with mass balance of PES-GO(0.6%) membrane taken into account.

One of the goals of DMF technology development is to concentrate wastewater for subsequent treatment by anaerobic digestion, which produces methane, a renewable energy source [57]. The theoretical potential for energy production from anaerobic digestion of the concentrate is shown in Figure 5 (assumed:1 g of COD yields 350 mL of $CH_4$ [58,59], and only 33% of methane energy is converted to electrical energy [60]). It is clear that the permeate recovery rate has a significant impact on DMF's energy recovery potential. Values greater than 80% would make it possible to recover up to 1.0 $kWh.m^{-3}$ of filtered wastewater, which would be sufficient to meet the technology's energy

demand, given that DMF full-scale energy consumption was estimated to be similar or lower than that consumed in an activated sludge system (0.3 to 0.6 kWh/$m^3$) [6,7].

Aside from sewage concentration, DMF technology contributes to water recovery and reuse. Depending on the water reuse application, a post-treatment may be required after the DMF process. For agricultural irrigation, the world largest water consumer, regulations and guidelines require a maximum and a minimum turbidity and COD of 14-0.2 NTU and 500-40 mg/L, respectively [61]. For PES-GO membranes, a high quality permeates with COD less than 30 mg/L and turbidity less than 0.5 NTU were obtained, allowing the water reuse after disinfection process and assurance of biologically and chemically safety in some agricultural irrigation applications, such as fiber crops, corn oil crops, and pastures irrigation [61].

### 3.3. Membrane fouling

#### 3.3.1 Filterability

Table 5 and Figure 6 show the initial and normalized flows during filtration tests for each membrane. PES membrane had a greater flux reduction during direct wastewater filtration than PES-GO membranes. In first cycle, the flux of all membranes decreases similarly and rapidly until approximately 80% of normalized flux. Following that, a distinct behavior is observed between the flux of PES and PES-GO membranes. While the flux decay rate for the PES-GO membranes is clearly reduced, the permeate flux decay for the PES membrane remains high up to approximately 50% of normalized flux. In the second wastewater filtration cycle (i.e., after physical cleaning), the difference in flow behavior between the membranes is even more pronounced. PES membrane exhibits a greater loss of flow than PES-GO at the start of filtration. Membranes incorporating GO, on the other hand, maintained a flow behavior similar to the first cycle, particularly

for the membrane with the highest amount of nanoparticles, indicating that adding GO is beneficial for maintaining their properties after physical cleaning (i.e., better reusability).

Despite the PES control membrane higher permeability, the permeate flux at the pseudo steady-state was close (Table 5), with the flux of the PES-GO membranes being slightly higher. PES membrane achieved 24% and 23% of the initial flux in the first and second filtration, respectively (initial flux: 117 LMH). For PES-GO membranes, the PES-GO(0.3%) had the lowest flux decrease in both filtration cycles, reaching 57% and 51% of the initial flux in the first and second, respectively (initial flux: 59 LMH), while the PES-GO(0.6%) reached 47% for both filtrations. This result indicates that the decrease in permeability caused by the higher concentration of GO in the polymer matrix had no negative effect on the permeate flux during direct filtration of wastewater, and that the type of fouling and its interaction with the membrane has a greater impact on permeate maintenance.

**Table 5:** Initial and final flux values during wastewater filtering, with percentages in brackets referring to the first cycle initial value.

| Membrane | Flux (1st cycle) | | Flux (2nd cycle) | |
|---|---|---|---|---|
| | Initial | Final | Initial | Final |
| PES | 150 | 36 (24%) | 117 | 34 (23%) |
| PES-GO(0.3%) | 71 | 38 (53%) | 59 | 36 (51%) |
| PES-GO(0.6%) | 79 | 37 (47%) | 72 | 37 (47%) |

It should also be noted that, while the better-normalized flux for GO-based membranes has been reported for model solution filtration, the flux behavior observed in this study follows the same trend, that is, significantly less decay for PES-GO membranes. For example, Igbinigun et al. [30] achieved lesser flux decay with PES-GO membranes (GO

content: 2, 4 and 6%) compared to a commercial PES membrane, with a final normalized flux of approximately 65% with 2 and 4% GO content and only ~20% with PES. It demonstrates that GO addition preserves its benefits in a complex matrix like raw municipal wastewater, which, when combined with the improved reusability of the PES-GO membrane, would maintain higher fluxes after several cycles of organic material concentration. The extent and significance of this result is further demonstrated by the findings of Gong et al. [55], who showed a great loss of permeability (from 110 LMHbar to 10 LMHbar) after 800 h of operation with a commercial PVDF membrane for organic matter up-concentration from wastewater.

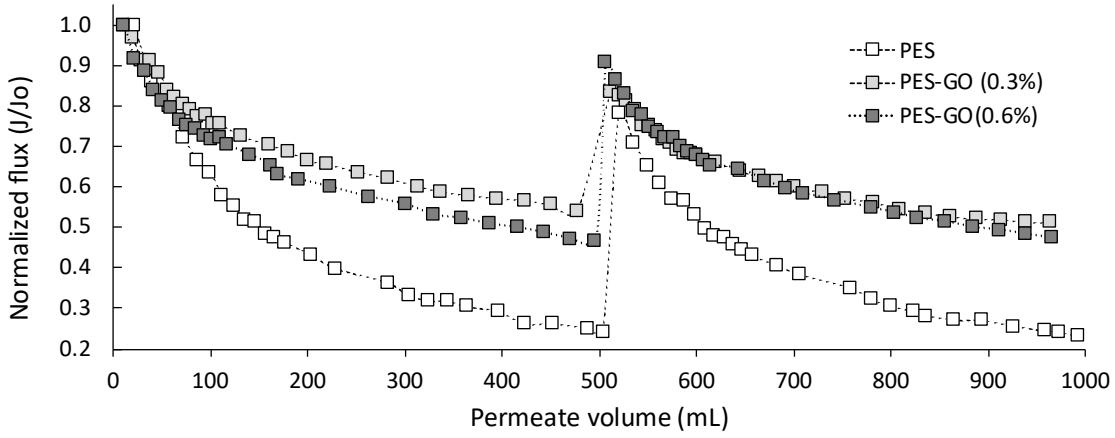


**Figure 6:** Normalized fluxes during filtration assays for the same volume of permeate.

### 3.3.2 Fouling mechanism and flux recovery

The standard (t/V-t) and classical cake (t/V-V) filtration models were applied to better understand the fouling behavior on the membrane surface, and the results are shown in Table 6. Despite the high correlation also obtained with the standard filtration model, the $R^2$ was higher for the classical cake filtration, indicating a better fit in this model and that cake formation is the main fouling mechanism (1 h of filtration testing). The data shows a fast decrease in flux during early filtration (Figure S3), most likely due to pore obstruction caused by foulant deposition and adsorption, followed by the formation of a cake layer on the membrane surface, as expected for crossflow filtration [45,62,63]. The

curve slope also contributes to comparing fouling between membranes, as higher values imply greater cake layer resistance [64]. The highest slope was obtained with PES membranes and the lowest with PES-GO(0.3%), showing the modified membrane advantage in terms of fouling reduction.

**Table 6:** Results of Standard (t/V-t) and classical cake (t/V-V) filtration models.

| **Membrane** | **Standard filtration** | | **Classical cake filtration** | |
|---|---|---|---|---|
| | **Equation** | **$R^2$** | **Equation** | **$R^2$** |
| PES | $(t/V) = 1.24t + a1$ | 0.97 | $(t/V) = 0.16V + a1$ | 0.99 |
| PES-GO(0.3%) | $(t/V) = 0.70t + a2$ | 0.95 | $(t/V) = 0.11V + a1$ | 0.97 |
| PES-GO(0.6%) | $(t/V) = 0.79t + a3$ | 0.95 | $(t/V) = 0.12V + a1$ | 0.98 |

The PES membrane presents the highest total fouling resistance (6.08 x $10^{12}$ $m^{-1}$), almost double that observed for MMMs, and the highest resistances for all three divisions of fouling considered in this work (i.e., $R_c$, $R_b$ and $R_{cb}$). The results for the RIS model (Table S2) also show the greater influence of the cake layer on total fouling and the differences between fouling layers in each membrane. Cake resistance was the highest of all three resistances for all filtrations, collaborating to indicate the predominance of such fouling mechanism. Hube et al. [65] reported similar results, demonstrating that after initial intermediate pore blocking, cake layer resistance became the largest during direct microfiltration and ultrafiltration of primary sewage. Pore blocking resistance decreased as the GO content increased. The $R_b$ (0.328 x $10^{12}$ $m^{-1}$) value of the PES-GO(0.6%) membrane was nearly two and a half times lower than the $R_b$ of the PES membrane, corroborating the results in Fig. 7, that show a lower irreversible resistance for this membrane.

Figure 7 shows the flux recovery ratios and relative fouling contributions for all three membranes analyzed. The flux recovery ratio (Fig. 7-a) obtained with physical cleaning of the PES membrane surface was 63%, lower than the flux recovery for PES-GO(0.3%), 87%, and for PES-GO(0.6%), 91%, implying a higher antifouling performance of modified membranes. The FRR results obtained in this study with raw wastewater are consistent to most of those reported in the literature, which show flux recovery of 45% to 96% for GO-based UF membranes. The differences in FRR found in the literature are generally related to the type of solution and the amount of GO in the mixed matrix. Algamdi et al. [53], for example, demonstrated an increase in FRR from 77% to 95% with an increase in GO content after filtration of a humic acid solution, followed by simple washing with water. Abdel-Karim et al. [40], on the other hand, obtained FRR ranging from 45% to 65% depending on the amount of GO after filtration of a BSA solution followed by cleaning with DI water. The higher FRR observed in this study when compared to model solution filtration can be attributed to differences in the cake layer formed with the wastewater matrix and its efficiency acting as a pre-filter for internal fouling prevention.

In addition to FRR, fouling reversibility is a useful in interpreting the membrane antifouling behavior. Figure 7-b clearly shows that as GO increases, the irreversible fouling fraction decreases. While reversible fouling contributed only 54% of total fouling over the PES membrane, it increased from 71% to 83% in PES-GO(0.3%) and PES-GO(0.6%), respectively. The low contribution of the irreversible fraction to total fouling by GO-based membranes indicates that the foulants are weakly deposited on the membrane surface and can be easily removed by physical cleaning processes, lowering chemical costs, and increasing membrane life-spam.

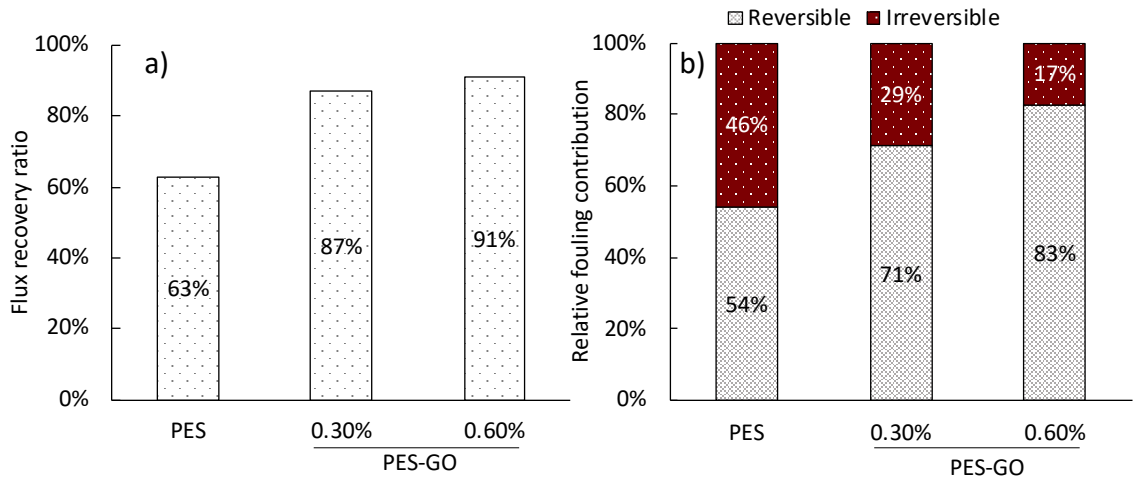


**Figure 7:** Flux recovery ratios (A) and relative fouling contributions (B) for filtration assays.

The differences in fouling behavior between PES and PES-GO membranes can be justified by the changes in pore size and permeability discussed in section 3.1, which have a strong impact on fouling formation, since membranes with larger pore sizes might present higher permeability but are more susceptible to inner pore blockage promoted by foulants. On the other hand, for membranes with smaller pores, certain particles would only adhere to the membrane surface or become part of the cake layer due to size exclusion [66–68]. Moreover, the better PES-GO membranes performance may be attributed to their higher hydrophilicity and more negative zeta potential. The contact angle results show that PES-GO membranes have lower hydrophobicity, implying weaker attachment of hydrophobic compounds to the membrane surface and pores. With less interaction between the membrane and foulants, adsorptive fouling is reduced, and shear stress caused on membrane surface can easily remove such compounds [24,69]. Furthermore, the presence of GO functional groups reduces the membrane zeta potential, increasing electrostatic repulsion of negatively charged foulants which contributes to an easier removal of foulants by physical methods. Besides, GO addition can make the membrane surface smoother, with lower roughness and fewer sites where foulants could

potentially get attached [70]. These advantages will lead to less frequent chemical cleaning for flux recovery (e.g., sodium hypochlorite, sodium hydroxide).

### 3.3.3 Fouling composition

The cake layer could be visualized by the SEM top surface images of PES and PES-GO fouled membranes (Fig. 8-a-c). In order to further study their composition, FTIR analyses of the membranes before and after fouling were performed (Fig. 8-d-f). FTIR spectra of PES and PES-GO membranes exhibit the characteristic peaks of the polymer which includes those at 1577 and 1484 $cm^{-1}$ associated to the C=C of the aromatic ring as well as those at 1320 and 1155 $cm^{-1}$ corresponding to the S=O stretching of the sulfonic group. In addition, the peak showed at 1241 $cm^{-1}$ refers to the C-O stretching of the polymer ether groups [71,72]. On the other hand, most of these peaks are overlapped in the spectra of the fouled membranes (F-PES and F-PES-GOs) due to the presence of organic compounds of the cake layer. FTIR spectra of the F-PES and F-PES-GOs show characteristic peaks of protein secondary structures, known as amide I (stretching vibrations of C=O and C-N at 1652 $cm^{-1}$) and amide II (N–H bending and C-N stretching at 1554 $cm^{-1}$) [73–75]. F-PES and F-PES-GOs spectra also exhibit a broad band centered at 3301 $cm^{-1}$ and a strong peak at 1054 $cm^{-1}$ related to O-H and C-O bonds stretching, respectively, which are characteristic of polysaccharides or polysaccharide-like substances [76]. Moreover, the sharp peaks in the vicinity of 2923 $cm^{-1}$ corresponds to C-H bonds of long linear aliphatic chains [77,78].

Influence of carbohydrates (mainly polysaccharides) and proteins over fouling is extensively described in literature [63,79]. Polysaccharides can cause severe irreversible fouling in microfiltration due to internal pore blockage or/and formation of a gel layer over membrane surface, resultant of polysaccharide crosslinks in the presence of cations, such as $Ca^{2+}$ [79,80]. The adsorption on membrane surface should also be considered. It

has been shown that foulant polysaccharides show great adsorption to phenyl groups, which are present in PES. On the other hand, the presence of carboxylic and (mainly) hydroxyl groups over PES-GO membrane surface should prevent such adsorption phenomenon [81,82]. Besides, the beneficial effect of enhanced hydrophilicity also reduces polysaccharides adsorption [83].

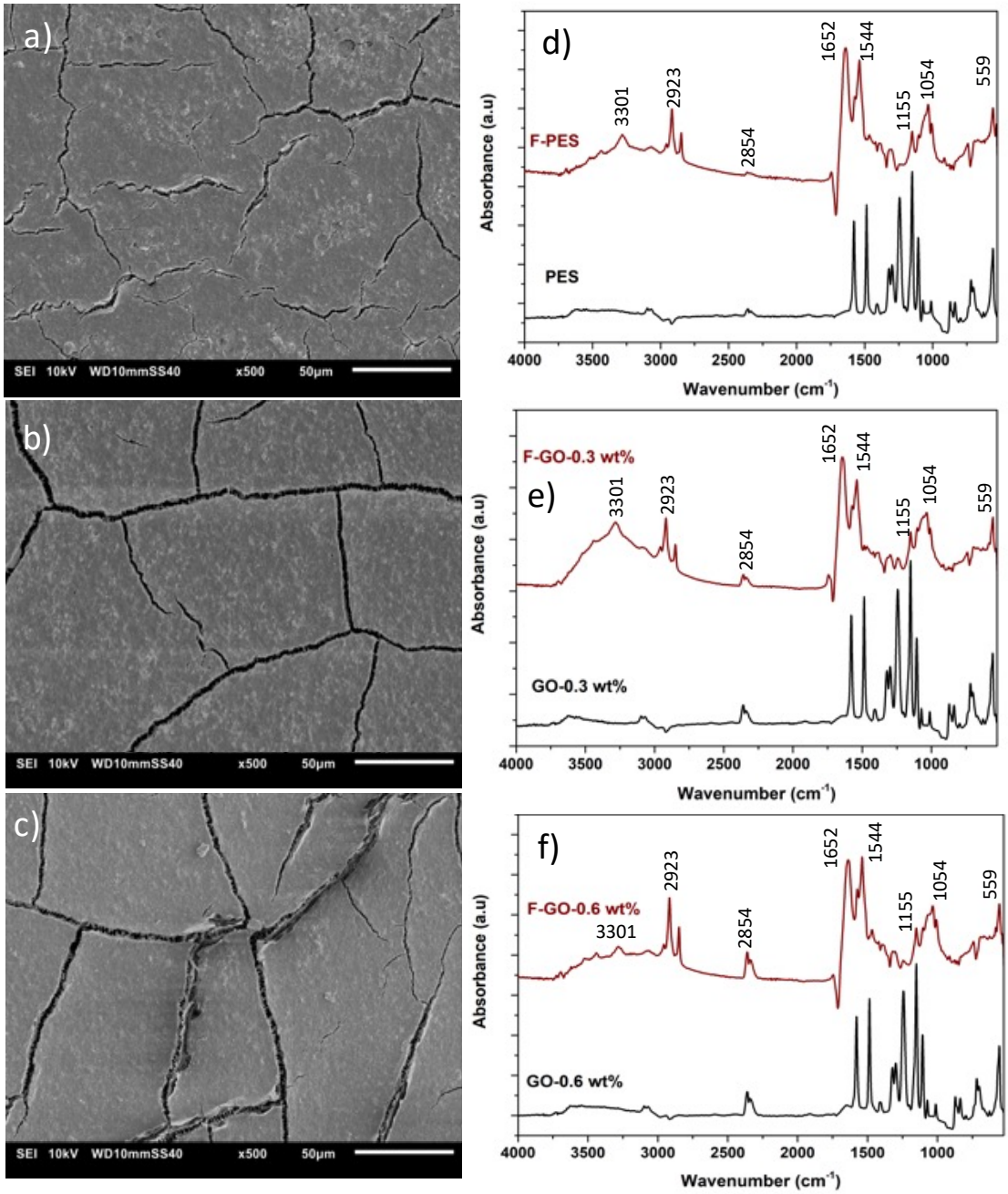


**Figure 8.** SEM images (a, b, c) and FTIR spectra (d, e, f) of the external fouling layer of the fouled membranes.

Similarly, protein fouling is mainly related with hydrophobic and electrostatic interactions between their functional groups (e.g. -OH, COOH and $-NH_2$) and membrane surface. This is because certain groups like phenyl, present in PES, are more prone to protein adsorption, resulting in irreversible fouling and strongly collaborating to cake layer formation [81,84]. Recent works with model proteins (BSA) show lower flux decays for PES-GO membranes [14,40] due to their strong presence of hydroxyl groups and enhanced hydrophilicity, which minimize the protein attachment [29,85].

To clarify the cake layer composition, proteins and carbohydrates over membrane surface were quantified and presented in Figure 9-a. The amount of carbohydrates increased from $0.14 \pm 0.01$ g/m$^2$ for PES to 0.17 and 0.18 g/m$^2$ for PES-GO(0.3%) and PES-GO(0.6%), respectively. However, the amount of proteins deposited differed for each membrane, with a higher value obtained for PES membrane surface ($1.16 \pm 0.03$ g/m$^2$) and the lower value for PES-GO(0.3%) ($0.71 \pm 0.07$ g/m$^2$).

The results of carbohydrates and proteins deposited on membrane surfaces are even more important when they are associated with the membranes rejection capacity. As previously demonstrated (Fig. 4), the MMMs had higher rejection efficiencies for both foulants (i.e., proteins and carbohydrates) than PES. PES-GO membranes, for example, were able to reject 28% more carbohydrates from sewage (Table 4), which explains the 21% and 28% increases in this compound in the fouling layers of PES-GO(0.3%) and PES-GO(0.6%), respectively. Protein, on the other hand, demonstrated a different trend. Even though PES-GO membranes rejected more protein, the concentration of protein in the cake layer of these membranes was lower. Furthermore, the quantification of these foulants revealed higher amounts of proteins than carbohydrates compared to those in the raw wastewater (Fig. 9-b). The P/C ratio increased from 2.7 in raw wastewater to 8.0 in

the cake layer of the PES membrane, and the same trend was seen in the PES-GO membranes (P/C ratio - 4.1 and 5.4), though to a lesser extent.

Although the reduction of protein deposited does not follow the amount of GO, these findings strongly suggest that changes in the membranes surface caused by the addition of GO allowed for a reduction in protein deposition, and its contribution to fouling formation during DMF is greater than carbohydrates. Despite that, further research is needed to investigate quantitatively adsorption and internal pore blockage caused by this foulant.

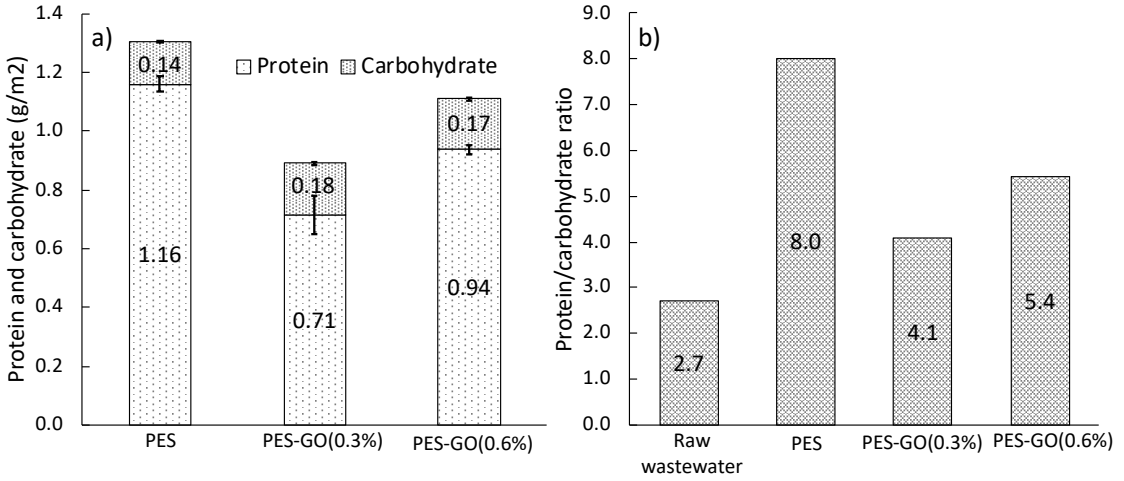


**Figure 9**: Protein and carbohydrate removed from cake layer (a) and protein/ carbohydrate ratio (b).

## 4. Conclusions

The addition of nanoparticles significantly alters the physicochemical properties of the polymeric membranes, making selective layer more hydrophilic, preventing the deposition of hydrophobic compounds and increasing rejection capacity. In this study, we show that PES membranes synthesized with concentrations of GO did not lead to greater permeate flux, but improved membrane reusability, flux recovery and a substantial increase of reversible fouling resistance when applied in DMF of municipal wastewater. The main foulant present in the cake layer was protein, and the addition of GO was able to reduce its deposition. Membrane selectivity was enhanced, resulting in higher rejection

of colloidal and dissolved compounds, with lower concentrations of compounds in the permeate that have little effect on COD but may be related to other micropollutants. In terms of COD recovery, there were no differences between the membranes, and no gain was observed for energy production through anaerobic digestion of organic material. However, the synthesized membranes showed high organic matter recovery, 1,950 mg of COD/L, for 90% of permeate recovery, exceeding anaerobic digestion minimum concentration, for methane production, aiming energy sustainability of the wastewater treatment plant. Since a higher quality of permeate was obtained, future research studies should investigate the organic micropollutants removal and its application in water reuse. Besides, the higher reversibility of the fouling layer on the membrane due to addition of GO, open possibilities for the use of more straightforward physical cleaning methods, including non-abrasive granular cleaning materials, to assist the fouling control and enhance the energy efficiency of this novel and promising conception of sewage treatment and resources recovery.

**Acknowledgment**

The authors wish to thank the Multiuser Experimental Central of UFABC (CEM-UFABC) for all laboratories, equipment and reagents made available for the accomplishment of this research. The authors wish to thank the São Paulo Research Foundation (FAPESP) (Grant number: 2016/23684-0 and 2020/11059-0) and CNPq (Grant number: 167185/2018-7).

**References**

[1] E.L. Subtil, R. Rodrigues, I. Hespanhol, J.C. Mierzwa, Water reuse potential at heavy-duty vehicles washing facilities – The mass balance approach for conservative contaminants, J. Clean. Prod. 166 (2017). https://doi.org/10.1016/j.jclepro.2017.08.162.

[2] Y. Luo, P. Le-Clech, R.K. Henderson, Simultaneous microalgae cultivation and wastewater treatment in submerged membrane photobioreactors: A review, Algal Res. 24 (2017) 425–437. https://doi.org/10.1016/j.algal.2016.10.026.

[3] G.M.F. Pierangeli, R.A. Ragio, R.F. Benassi, G.B. Gregoracci, E.L. Subtil, Pollutant removal, electricity generation and microbial community in an electrochemical membrane bioreactor during co-treatment of sewage and landfill leachate, J. Environ. Chem. Eng. 9 (2021) 2213–3437. https://doi.org/10.1016/J.JECE.2021.106205.

[4] V. Senatore, A. Buonerba, T. Zarra, G. Oliva, V. Belgiorno, J. Boguniewicz-Zablocka, V. Naddeo, Innovative membrane photobioreactor for sustainable CO2 capture and utilization, Chemosphere. 273 (2021) 129682. https://doi.org/10.1016/j.chemosphere.2021.129682.

[5] T.A. Nascimento, F. Fdz-Polanco, M. Peña, Membrane-Based Technologies for the Up-Concentration of Municipal Wastewater: A Review of Pretreatment Intensification, Sep. Purif. Rev. 49 (2018) 1–19. https://doi.org/10.1080/15422119.2018.1481089.

[6] K. Kimura, M. Yamakawa, A. Hafuka, Direct membrane filtration (DMF) for recovery of organic matter in municipal wastewater using small amounts of chemicals and energy, Chemosphere. 277 (2021) 130244. https://doi.org/10.1016/j.chemosphere.2021.130244.

[7] T.A. Nascimento, M.P. Miranda, Continuous municipal wastewater up-concentration by direct membrane filtration, considering the effect of intermittent gas scouring and threshold flux determination, J. Water Process Eng. 39 (2021) 101733. https://doi.org/10.1016/j.jwpe.2020.101733.

[8] S. Hube, M. Eskafi, K. Fríða Hrafnkelsdóttir, B. Bjarnadóttir, M. Ásta Bjarnadóttir,

S. Axelsdóttir, B. Wu, Direct membrane filtration for wastewater treatment and resource recovery: A review, Sci. Total Environ. 710 (2020). https://doi.org/10.1016/j.scitotenv.2019.136375.

[9] H. Gong, Z. Jin, H. Xu, Q. Yuan, J. Zuo, J. Wu, K. Wang, Enhanced membrane-based pre-concentration improves wastewater organic matter recovery: Pilot-scale performance and membrane fouling, J. Clean. Prod. 206 (2019) 307–314. https://doi.org/10.1016/j.jclepro.2018.09.209.

[10] K. Kimura, D. Honoki, T. Sato, Effective physical cleaning and adequate membrane flux for direct membrane filtration (DMF) of municipal wastewater: Up-concentration of organic matter for efficient energy recovery, Sep. Purif. Technol. 181 (2017) 37–43. https://doi.org/10.1016/j.seppur.2017.03.005.

[11] T.A. Nascimento, M.P. Miranda, Control strategies for the long-term operation of direct membrane filtration of municipal wastewater, J. Environ. Chem. Eng. 9 (2021) 105335. https://doi.org/10.1016/j.jece.2021.105335.

[12] H. Gong, Z. Jin, X. Wang, K. Wang, Membrane fouling controlled by coagulation/adsorption during direct sewage membrane filtration (DSMF) for organic matter concentration, J. Environ. Sci. (China). 32 (2015) 1–7. https://doi.org/10.1016/j.jes.2015.01.002.

[13] E.L. Subtil, J. Gonçalves, H.G. Lemos, E.C. Venancio, J.C. Mierzwa, J. dos Santos de Souza, W. Alves, P. Le-Clech, Preparation and characterization of a new composite conductive polyethersulfone membrane using polyaniline (PANI) and reduced graphene oxide (rGO), Chem. Eng. J. 390 (2020) 124612. https://doi.org/10.1016/j.cej.2020.124612.

[14] H.G. Lemos, R.A. Ragio, A.C.S. Conceição, E.C. Venancio, J.C. Mierzwa, E.L. Subtil, Assessment of mixed matrix membranes (MMMs) incorporated with

graphene oxide (GO) for co-treatment of wastewater and landfill leachate (LFL) in a membrane bioreactor (MBR), Chem. Eng. J. 425 (2021). https://doi.org/10.1016/j.cej.2021.131772.

[15] J. Gonçalves, A.A. Baldovi, B. Chyoshi, L. Zanata, A.M. Salcedo, E.L. Subtil, L.H.G. Coelho, Effect of aluminum sulfate and cationic polymer addition in the mixed liquor of a submerged membrane bioreactor (smbr): sludge characteristics and orthophosphate removal in batch experiments, Brazilian J. Chem. Eng. 36 (n.d.) 693–703. https://doi.org/10.1590/0104-6632.20190362s20180128.

[16] E.L. Subtil, M.V. Silva, B.A. Lotto, M.R.D. Moretto, J.C. Mierzwa, Pilot-scale investigation on the feasibility of simultaneous nitrification and denitrification (SND) in a continuous flow single-stage membrane bioreactor, J. Water Process Eng. 32 (2019). https://doi.org/10.1016/j.jwpe.2019.100995.

[17] Z. Jin, H. Gong, H. Temmink, H. Nie, J. Wu, J. Zuo, K. Wang, Efficient sewage pre-concentration with combined coagulation microfiltration for organic matter recovery, Chem. Eng. J. 292 (2016) 130–138. https://doi.org/10.1016/j.cej.2016.02.024.

[18] B.C. Huang, Y.F. Guan, W. Chen, H.Q. Yu, Membrane fouling characteristics and mitigation in a coagulation-assisted microfiltration process for municipal wastewater pretreatment, Water Res. 123 (2017) 216–223. https://doi.org/10.1016/j.watres.2017.06.080.

[19] Z. Jin, F. Meng, H. Gong, C. Wang, K. Wang, Improved low-carbon-consuming fouling control in long-term membrane-based sewage pre-concentration: The role of enhanced coagulation process and air backflushing in sustainable sewage treatment, J. Memb. Sci. 529 (2017) 252–262. https://doi.org/10.1016/j.memsci.2017.02.009.

[20] S. Hube, J. Wang, L. Nuang Sim, T. Haur Chong, B. Wu, Direct membrane filtration of municipal wastewater: Linking periodical physical cleaning with fouling mechanisms, Sep. Purif. Technol. 259 (2021) 118125. https://doi.org/10.1016/j.seppur.2020.118125.

[21] J. Zhao, Y. Yang, C. Li, L.-A. Hou, Fabrication of GO modified PVDF membrane for dissolved organic matter removal: Removal mechanism and antifouling property, Sep. Purif. Technol. 209 (2018) 482–490. https://doi.org/10.1016/j.seppur.2018.07.050.

[22] M. Ahsani, H. Hazrati, M. Javadi, M. Ulbricht, R. Yegani, Preparation of antibiofouling nanocomposite PVDF/Ag-SiO 2 membrane and long-term performance evaluation in the MBR system fed by real pharmaceutical wastewater, Sep. Purif. Technol. 249 (2020) 116938. https://doi.org/10.1016/j.seppur.2020.116938.

[23] Y. Jiang, Q. Zeng, P. Biswas, J.D. Fortner, Graphene oxides as nanofillers in polysulfone ultrafiltration membranes: Shape matters, (2019). https://doi.org/10.1016/j.memsci.2019.03.056.

[24] L. Yong Ng, H. Syean Chua, C. Yin Ng, Incorporation of graphene oxide-based nanocomposite in the polymeric membrane for water and wastewater treatment: A review on recent development, J. Environ. Chem. Eng. 9 (2021) 2213–3437. https://doi.org/10.1016/j.jece.2021.105994.

[25] M. Fathizadeh, W.L. Xu, M. Shen, E. Jeng, F. Zhou, Q. Dong, D. Behera, Z. Song, L. Wang, A. Shakouri, K. Khivantsev, M. Yu, Environmental Science Water Research & Technology Antifouling UV-treated GO/PES hollow fiber membranes in a membrane bioreactor (MBR) †, Environ. Sci. Water Res. Technol. 5 (2019) 1244. https://doi.org/10.1039/c9ew00217k.

[26] H. Ravishankar, S. Moazzem, V. Jegatheesan, Performance evaluation of A2O MBR system with graphene oxide (GO) blended polysulfone (PSf) composite membrane for treatment of high strength synthetic wastewater containing lead, Chemosphere. 234 (2019) 148–161. https://doi.org/10.1016/j.chemosphere.2019.05.264.

[27] S. Ayyaru, Y.-H. Ahn, Application of sulfonic acid group functionalized graphene oxide to improve hydrophilicity, permeability, and antifouling of PVDF nanocomposite ultrafiltration membranes, J. Memb. Sci. 525 (2016) 210–219. https://doi.org/10.1016/j.memsci.2016.10.048.

[28] S. Zinadini, V. Vatanpour, A.A. Zinatizadeh, M. Rahimi, Z. Rahimi, M. Kian, Preparation and characterization of antifouling graphene oxide/polyethersulfone ultrafiltration membrane: Application in MBR for dairy wastewater treatment, J. Water Process Eng. 7 (2015) 280–294. https://doi.org/10.1016/j.jwpe.2015.07.005.

[29] F. Jin, W. Lv, C. Zhang, Z. Li, R. Su, W. Qi, Q.-H. Yang, Z. He, High-performance ultrafiltration membranes based on polyethersulfone–graphene oxide composites, RSC Adv. 3 (2013) 21394–21397. https://doi.org/10.1039/C3RA42908C.

[30] E. Igbinigun, Y. Fennell, R. Malaisamy, K.L. Jones, V. Morris, Graphene oxide functionalized polyethersulfone membrane to reduce organic fouling, J. Memb. Sci. 514 (2016) 518–526. https://doi.org/10.1016/j.memsci.2016.05.024.

[31] W.M.K.R.T.W. Bandara, H. Satoh, M. Sasakawa, Y. Nakahara, M. Takahashi, S. Okabe, Removal of residual dissolved methane gas in an upflow anaerobic sludge blanket reactor treating low-strength wastewater at low temperature with degassing membrane, Water Res. 45 (2011) 3533–3540. https://doi.org/10.1016/J.WATRES.2011.04.030.

[32] G.S. Arcanjo, F.C.R. Costa, B.C. Ricci, A.H. Mounteer, E.N.M.L. de Melo, B.F. Cavalcante, A. V. Araújo, C. V. Faria, M.C.S. Amaral, Draw solution solute selection for a hybrid forward osmosis-membrane distillation module: Effects on trace organic compound rejection, water flux and polarization, Chem. Eng. J. 400 (2020) 125857. https://doi.org/10.1016/j.cej.2020.125857.

[33] Y. Gao, Z. Fang, P. Liang, X. Huang, Direct concentration of municipal sewage by forward osmosis and membrane fouling behavior, Bioresour. Technol. 247 (2018) 730–735. https://doi.org/10.1016/J.BIORTECH.2017.09.145.

[34] E.L. Subtil, S.T.A. Cassini, R.F. Gonçalves, Sulfate and dissolved sulfide variation under low COD/Sulfate ratio in Up-flow Anaerobic Sludge Blanket (UASB) treating domestic wastewater, Ambient. e Agua - An Interdiscip. J. Appl. Sci. 7 (2012) 130–139. https://doi.org/10.4136/ambi-agua.849.

[35] D.C. Marcano, D. V. Kosynkin, J.M. Berlin, A. Sinitskii, Z. Sun, A. Slesarev, L.B. Alemany, W. Lu, J.M. Tour, Improved synthesis of graphene oxide, ACS Nano. 4 (2010) 4806–4814. https://doi.org/10.1021/nn1006368.

[36] S.X. Liu, J.T. Kim, Characterization of Surface Modification of Polyethersulfone Membrane, J. Adhes. Sci. Technol. 25 (2012) 193–212. https://doi.org/10.1163/016942410X503311.

[37] J.C. Mierzwa, M.C.C. da Silva, L.R.V. Veras, E.L. Subtil, R. Rodrigues, T. Li, K.R. Landenberger, Enhancing spiral-wound ultrafiltration performance for direct drinking water treatment through operational procedures improvement: A feasible option for the Sao Paulo Metropolitan Region, Desalination. 307 (2012). https://doi.org/10.1016/j.desal.2012.09.006.

[38] I. Cisse, S. Oakes, S. Sachdev, M. Toro, S. Lutondo, D. Shedden, K.M. Atkinson, J. Shertok, M. Mehan, S.K. Gupta, G.A. Takacs, Surface Modification of

Polyethersulfone (PES) with UV Photo-Oxidation, (2021). https://doi.org/10.3390/technologies9020036.

[39] N. Hilal, A.F. Ismail, T. Matsuura, D. Oatley-Radcliffe, Membrane Characterization, Elsevier, Amsterdam, 2017. https://doi.org/10.1007/978-0-387-78991-0_6.

[40] A. Abdel-Karim, S. Leaper, M. Alberto, A. Vijayaraghavan, X. Fan, S.M. Holmes, E.R. Souaya, M.I. Badawy, P. Gorgojo, High flux and fouling resistant flat sheet polyethersulfone membranes incorporated with graphene oxide for ultrafiltration applications, Chem. Eng. J. 334 (2018) 789–799. https://doi.org/10.1016/j.cej.2017.10.069.

[41] APHA, AWWA, WEF, Standard Methods for Examination of Water and Wastewater, Washingt. Am. Public Heal. Assoc. (2012).

[42] A.A. Albalasmeh, A.A. Berhe, T.A. Ghezzehei, A new method for rapid determination of carbohydrate and total carbon concentrations using UV spectrophotometry, Carbohydr. Polym. 97 (2013) 253–261. https://doi.org/10.1016/j.carbpol.2013.04.072.

[43] O. Lowry, H. Schagger, W.A. Cramer, G. Vonjagow, Protein Measurement with the folin phenol reagent, Anal. Biochem. 217 (1994).

[44] R.A. Ragio, L.F. Miyazaki, M.A. De Oliveira, L.H.G. Coelho, R.D.F. Bueno, E.L. Subtil, Pre-coagulation assisted ultrafiltration membrane process for anaerobic effluent, J. Environ. Chem. Eng. 8 (2020) 104066. https://doi.org/10.1016/j.jece.2020.104066.

[45] H.-D. Park, I.-S. Chang, K.-J. Lee, Principles of Membrane Bioreactors for Wastewater Treatment, 2015. https://doi.org/10.1201/b18368.

[46] M.H. Al-Malack, A.A. Bukhari, N.S. Abuzaid, Crossflow microfiltration of

electrocoagulated kaolin suspension: fouling mechanism, J. Memb. Sci. 243 (2004) 143–153. https://doi.org/https://doi.org/10.1016/j.memsci.2004.05.032.

[47] V. Vatanpour, S.S. Madaeni, R. Moradian, S. Zinadini, B. Astinchap, Fabrication and characterization of novel antifouling nanofiltration membrane prepared from oxidized multiwalled carbon nanotube/polyethersulfone nanocomposite, J. Memb. Sci. 375 (2011) 284–294. https://doi.org/10.1016/j.memsci.2011.03.055.

[48] G. Di Bella, D. Di Trapani, A Brief Review on the Resistance-in-Series Model in Membrane Bioreactors (MBRs), Membranes (Basel). 9 (2019). https://doi.org/10.3390/membranes9020024.

[49] G. Di Bella, F. Durante, M. Torregrossa, G. Viviani, P. Mercurio, A. Cicala, The role of fouling mechanisms in a membrane bioreactor, Water Sci. Technol. 55 (2007) 455–464. https://doi.org/10.2166/wst.2007.290.

[50] P. Walstra, J.T.M. Wouters, T.J. Geurts, Dairy science and technology, second edition, 2005.

[51] B.E. Logan, G.A. Wagenseller, Molecular Size Distributions of Dissolved Organic Matter in Wastewater Transformed by Treatment in a Full-Scale Trickling Filter, Water Environ. Res. 72 (2000) 277–281. https://doi.org/https://doi.org/10.2175/106143000X137482.

[52] A. Maartens, P. Swart, E.P. Jacobs, Humic membrane foulants in natural brown water: characterization and removal, Desalination. 115 (1998) 215–227. https://doi.org/10.1016/S0011-9164(98)00041-1.

[53] M. Saad Algamdi, I.H. Alsohaimi, J. Lawler, H.M. Ali, A.M. Aldawsari, H.M.A. Hassan, Fabrication of graphene oxide incorporated polyethersulfone hybrid ultrafiltration membranes for humic acid removal, Sep. Purif. Technol. 223 (2019) 17–23. https://doi.org/10.1016/j.seppur.2019.04.057.

[54] M. Hu, Z. Cui, J. Li, L. Zhang, Y. Mo, D.S. Dlamini, H. Wang, B. He, J. Li, H. Matsuyama, Ultra-low graphene oxide loading for water permeability, antifouling and antibacterial improvement of polyethersulfone/sulfonated polysulfone ultrafiltration membranes, J. Colloid Interface Sci. 552 (2019) 319–331. https://doi.org/10.1016/J.JCIS.2019.05.065.

[55] H. Gong, Z. Jin, H. Xu, Q. Yuan, J. Zuo, J. Wu, K. Wang, Enhanced membrane-based pre-concentration improves wastewater organic matter recovery: Pilot-scale performance and membrane fouling, J. Clean. Prod. 206 (2019) 307–314. https://doi.org/10.1016/j.jclepro.2018.09.209.

[56] J.C. Ortega-Bravo, J. Pavez, V. Hidalgo, I. Reyes-Caniupán, Á. Torres-Aravena, D. Jeison, Biogas Production from Concentrated Municipal Sewage by Forward Osmosis, Micro and Ultrafiltration, Sustain. 2022, Vol. 14, Page 2629. 14 (2022) 2629. https://doi.org/10.3390/SU14052629.

[57] J.C. Ortega-Bravo, G. Ruiz-Filippi, A. Donoso-Bravo, I.E. Reyes-Caniupán, D. Jeison, Forward osmosis: Evaluation thin-film-composite membrane for municipal sewage concentration, Chem. Eng. J. 306 (2016) 531–537. https://doi.org/https://doi.org/10.1016/j.cej.2016.07.085.

[58] T.Z. Macedo, H. de Souza Dornelles, A.L. do Valle Marques, T. PalladinoDelforno, V.B. Centurion, V.M. de Oliveira, E.L. Silva, M.B.A. Varesche, The influence of upflow velocity and hydraulic retention time changes on taxonomic and functional characterization in Fluidized Bed Reactor treating commercial laundry wastewater in co-digestion with domestic sewage, Biodegradation. 31 (2020) 73–89. https://doi.org/10.1007/s10532-020-09895-x.

[59] M. Lesteur, V. Bellon-Maurel, C. Gonzalez, E. Latrille, J.M. Roger, G. Junqua, J.P. Steyer, Alternative methods for determining anaerobic biodegradability: A

review, Process Biochem. 45 (2010) 431–440. https://doi.org/https://doi.org/10.1016/j.procbio.2009.11.018.

[60] J. Kim, K. Kim, H. Ye, E. Lee, C. Shin, P.L. McCarty, J. Bae, Anaerobic Fluidized Bed Membrane Bioreactor for Wastewater Treatment, Environ. Sci. Technol. 45 (2011) 576–581. https://doi.org/10.1021/es1027103.

[61] F. Shoushtarian, M. Negahban-Azar, Worldwide Regulations and Guidelines for Agricultural Water Reuse: A Critical Review, Water. 12 (2020). https://doi.org/10.3390/w12040971.

[62] T.-H. Bae, T.-M. Tak, Interpretation of fouling characteristics of ultrafiltration membranes during the filtration of membrane bioreactor mixed liquor, J. Memb. Sci. 264 (2005) 151–160. https://doi.org/https://doi.org/10.1016/j.memsci.2005.04.037.

[63] P. Le-Clech, V. Chen, T.A.G. Fane, Fouling in membrane bioreactors used in wastewater treatment, J. Memb. Sci. 284 (2006) 17–53. https://doi.org/https://doi.org/10.1016/j.memsci.2006.08.019.

[64] C. Zhao, X. Xu, J. Chen, G. Wang, F. Yang, Highly effective antifouling performance of PVDF/graphene oxide composite membrane in membrane bioreactor (MBR) system, Desalination. 340 (2014) 59–66. https://doi.org/10.1016/j.desal.2014.02.022.

[65] S. Hube, J. Wang, L.N. Sim, D. Dagmar´ Dagmar´olafsdóttir, H. Chong, B. Wu, Fouling and mitigation mechanisms during direct microfiltration and ultrafiltration of primary wastewater, J. Water Process Eng. 44 (2021) 2214–7144. https://doi.org/10.1016/j.jwpe.2021.102331.

[66] C.-F. Lin, A. Yu-Chen Lin, P. Sri Chandana, C.-Y. Tsai, Effects of mass retention of dissolved organic matter and membrane pore size on membrane fouling and flux

decline, Water Res. 43 (2009) 389–394. https://doi.org/https://doi.org/10.1016/j.watres.2008.10.042.

[67] M. Zielińska, M. Galik, Use of Ceramic Membranes in a Membrane Filtration Supported by Coagulation for the Treatment of Dairy Wastewater, Water, Air, Soil Pollut. 228 (2017) 173. https://doi.org/10.1007/s11270-017-3365-x.

[68] K.J. Howe, M.M. Clark, Effect of coagulation pretreatment on membrane filtration performance, J. AWWA. 98 (2006) 133–146. https://doi.org/https://doi.org/10.1002/j.1551-8833.2006.tb07641.x.

[69] S. Xia, M. Ni, Preparation of poly(vinylidene fluoride) membranes with graphene oxide addition for natural organic matter removal, J. Memb. Sci. 473 (2015) 54–62. https://doi.org/10.1016/j.memsci.2014.09.018.

[70] N. Meng, R. Claire, E. Priestley, Y. Zhang, H. Wang, X. Zhang, The effect of reduction degree of GO nanosheets on microstructure and performance of PVDF/GO hybrid membranes, J. Membr. Sci. J. 501 (2016) 169–178. https://doi.org/10.1016/j.memsci.2015.12.004.

[71] E.M. Deemer, T. Capt, O. Owoseni, T. Akter, W.S. Walker, Hypochlorite Resistant Graphene Oxide Incorporated Ultrafiltration Membranes with High Sustainable Flux, Ind. Eng. Chem. Res. 58 (2019) 11964–11975. https://doi.org/10.1021/acs.iecr.9b01685.

[72] K. Yadav, K. Morison, M.P. Staiger, Effects of hypochlorite treatment on the surface morphology and mechanical properties of polyethersulfone ultrafiltration membranes, Polym. Degrad. Stab. 94 (2009) 1955–1961. https://doi.org/10.1016/j.polymdegradstab.2009.07.027.

[73] M.J. Luján-Facundo, J.A. Mendoza-Roca, B. Cuartas-Uribe, S. Álvarez-Blanco, Evaluation of cleaning efficiency of ultrafiltration membranes fouled by BSA

using FTIR-ATR as a tool, (n.d.). https://doi.org/10.1016/j.jfoodeng.2015.04.015.

[74] W.J. Gao, H.J. Lin, K.T. Leung, H. Schraft, B.Q. Liao, Structure of cake layer in a submerged anaerobic membrane bioreactor, J. Memb. Sci. 374 (2011) 110–120. https://doi.org/https://doi.org/10.1016/j.memsci.2011.03.019.

[75] F. Meng, H. Zhang, F. Yang, L. Liu, Characterization of Cake Layer in Submerged Membrane Bioreactor, Environ. Sci. Technol. 41 (2007) 4065–4070. https://doi.org/10.1021/es062208b.

[76] H.J. Lin, K. Xie, B. Mahendran, D.M. Bagley, K.T. Leung, S.N. Liss, B.Q. Liao, Sludge properties and their effects on membrane fouling in submerged anaerobic membrane bioreactors (SAnMBRs), Water Res. 43 (2009) 3827–3837. https://doi.org/https://doi.org/10.1016/j.watres.2009.05.025.

[77] F. Mashayekhi, H. Hazrati, J. Shayegan, Fouling control mechanism by optimum ozone addition in submerged membrane bioreactors treating synthetic wastewater, J. Environ. Chem. Eng. 6 (2018) 7294–7301. https://doi.org/https://doi.org/10.1016/j.jece.2018.10.016.

[78] A. Yurtsever, E. Basaran, D. Ucar, E. Sahinkaya, Self-forming dynamic membrane bioreactor for textile industry wastewater treatment, Sci. Total Environ. 751 (2021) 141572. https://doi.org/https://doi.org/10.1016/j.scitotenv.2020.141572.

[79] F. Meng, S. Zhang, Y. Oh, Z. Zhou, H.S. Shin, S.R. Chae, Fouling in membrane bioreactors: An updated review, Water Res. 114 (2017) 151–180. https://doi.org/10.1016/j.watres.2017.02.006.

[80] S. Meng, H. Liu, Q. Zhao, N. Shen, M. Zhang, Filtration Performances of Different Polysaccharides in Microfiltration Process, Processes. 7 (2019). https://doi.org/10.3390/pr7120897.

[81] A.E. Contreras, Z. Steiner, J. Miao, R. Kasher, Q. Li, Studying the Role of

Common Membrane Surface Functionalities on Adsorption and Cleaning of Organic Foulants Using QCM-D, Environ. Sci. Technol. 45 (2011) 6309–6315. https://doi.org/10.1021/es200570t.

[82] J. Wu, A.E. Contreras, Q. Li, Studying the impact of RO membrane surface functional groups on alginate fouling in seawater desalination, J. Memb. Sci. 458 (2014) 120–127. https://doi.org/https://doi.org/10.1016/j.memsci.2014.01.056.

[83] Y. Zhang, Y. Wang, X. Cao, J. Xue, Q. Zhang, J. Tian, X. Li, X. Qiu, B. Pan, A.Z. Gu, X. Zheng, Effect of carboxyl and hydroxyl groups on adsorptive polysaccharide fouling: A comparative study based on PVDF and graphene oxide (GO) modified PVDF surfaces, J. Memb. Sci. 595 (2020) 117514. https://doi.org/https://doi.org/10.1016/j.memsci.2019.117514.

[84] X. Zheng, M.T. Khan, X. Cao, J.-P. Croue, Importance of origin and characteristics of biopolymers in reversible and irreversible fouling of ultrafiltration membranes, Sci. Total Environ. 784 (2021) 147157. https://doi.org/https://doi.org/10.1016/j.scitotenv.2021.147157.

[85] L. Yu, Y. Zhang, B. Zhang, J. Liu, H. Zhang, C. Song, Preparation and characterization of HPEI-GO/PES ultrafiltration membrane with antifouling and antibacterial properties, J. Memb. Sci. 447 (2013) 452–462. https://doi.org/https://doi.org/10.1016/j.memsci.2013.07.042.